Effect of the Viscosity Ratio, μ_d/μ_c, on the Particle-size Distribution in Emulsions

Shun'ichi TSUKIYAMA, Akira TAKAMURA, Yasuko FUKUDA, and Masumi KOISHI*

Meiji College of Pharmacy, 1-22-1, Yato-chō, Tanashi-shi, Tokyo 188

**Faculty of Pharmaceutical Sciences, Science University of Tokyo, Ichigaya Funakawara-machi, Shinjuku-ku, Tokyo 162*

(Received August 4, 1975)

The object of this paper is to investigate the effect of the ratio of the viscosities of dispersed and continuous phases, μ_d/μ_c, on the particle-size distribution in o/w-type emulsions. The viscosity ratios (μ_d/μ_c) used were 0.836 : 1, 0.271 : 1, 0.0992 : 1, 0.0280 : 1, and 0.00133 : 1. The size of the dispersed liquid droplets was measured by the microphotographic method. The mean diameter and the particle-size distribution were determined, and, further, the specific interfacial energy was evaluated. When the viscosity ratio was much smaller than unity, the particle-size distribution showed a skewed curve. On the contrary, the specific interfacial energy increased remarkably as the viscosity ratio approached unity.

Emulsion formation has, in general, been discussed from two different points of view[1] from the point of view of surface chemical[2] and from that of chemical engineering.[3] There are many factors which affect emulsion formation; the combination of two liquids, the mode of mixing two liquid phases, the concentration of the dispersed phase, the kind of emulsifying agent, the viscosity ratio of the two phases, the temperature, the equipment, the method of agitation, the impeller velocity, the agitation time, and so on.

In our previous papers,[4-6] statistical considerations of the experimental results were presented in connection with emulsion formation under various conditions. In those considerations, attempts were made to obtain the effects on emulsion formation of the kind and concentration of emulsifying agents, the energy efficiency of agitation,[5] and the agitation time. However, these studies were all undertaken without taking the viscosity factor into account.

In this paper, therefore, the effect of the ratio of the viscosities of the dispersed and continuous phases, μ_d/μ_c, on emulsion formation will be examined in relation to the particle-size distribution, the mean diameter of the dispersed phase, and the specific interfacial energy.

Experimental

Equipment. A sketch of the apparatus employed is shown in Fig. 1. The clear acrylate resin agitation tank with 4-baffles was 150 mmϕ in diameter and 210 mm deep. A stainless-steel agitation impeller of 49.00 mmϕ was of the standard Rushton type with 6-blades.[7] The tank was surrounded by a water jacket in order to keep the temperature of the liquid within it at 20.0 °C.

Measurement of Physical Properties. Mixtures of sodium silicate (Kishida Chemical Co.) and distilled water in varying ratios were used as the continuous phase. The total concentration of sodium silicate in the mixtures was varied from 17.0 to 88.0% (w/w). The dispersed phase was made up by mixing n-C_7H_{16} and CCl_4 in various volume ratios; the density was adjusted so as to be the same as that of the continuous phase (1.000—1.567 g/cm^3).

Tween-20 (Tōhō Chemical Industry Co.) was employed as the emulsifying agent; its concentration was 0.1% (w/w). The interfacial tensions were measured by the ring method,[8] and the viscosities of liquids, by the rotating viscometer[9] at

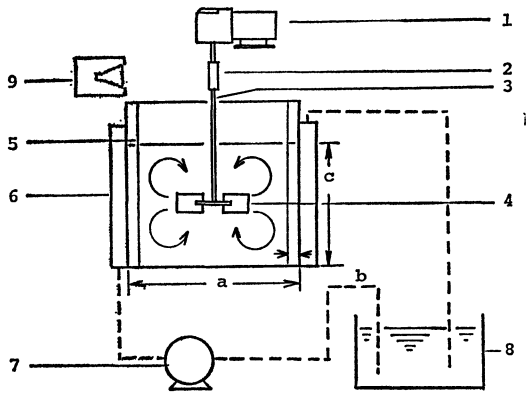

Fig. 1. Apparatus.

1 : motor 2 : toruqe meter 3 : shaft 4 : impeller
5 : baffle 6 : tank 7 : pump 8 : thermostat
9 : storobo scope.

TABLE 1. PHYSICAL PROPERTIES OF EACH CONTINUOUS PHASE

Concentration of Sodium Silicate (%, w/w)	Concentration of Tween-20 (%, w/w)	Density of continuous phase ρ_c (g/cm^3)	Density ratio ρ_d/ρ_c (—)	Viscosity of continuous phase μ_c (g/cm·s)	Viscosity ratio μ_d/μ_c (—)	Interfacial tension $\lvert\gamma_d-\gamma_c\rvert$ (dyn/cm)
0.0	0.1	1.000	1.000	1.005	8.36×10^{-1}	22.85
17.5	0.1	1.290	1.000	4.000	2.71×10^{-1}	15.50
58.0	0.1	1.400	1.000	12.20	9.92×10^{-2}	15.82
70.5	0.1	1.482	1.000	47.00	2.80×10^{-2}	18.03
88.0	0.1	1.567	1.000	1100	1.33×10^{-3}	21.58

Impeller diameter: 49.0 mm, Tank diameter: 150 mm, Revolution number: 330, 400, and 660 rpm.

20.0±0.1 °C.

The viscosity ratio, μ_d/μ_c, was widely varied from 0.836 : 1 to 0.00133 : 1. The concentration of sodium silicate, the density of the continuous phase, the density ratio, the viscosity of the continuous phase, the viscosity ratio, and the interfacial tension are summarized in Table 1.

Experimental Procedure. The experiments were carried out under the following conditions:

(1) The viscosity ratios, μ_d/μ_c, used were 0.836 : 1, 0.271 : 1, 0.0992 : 1, 0.0280 : 1, and 0.00133 : 1.

(2) The revolution rates were 330, 400, and 660 rpm.

(3) Samplings were made 5, 10, 20, 35, and 60 min after agitation has started.

The agitation tank was filled with 1960 ml of an aqueous sodium silicate solution, a continuous phase, containing Tween-20 as an emulsifying agent. The impeller was set in the center of the tank. On the middle of the impeller was gently placed 40 ml of a mixed solvent, a dispersed phase, as an almost perfect globule. The concentration of the dispersed phase was kept at 2.0% (v/v). The total liquid volume was, therefore, 2000 ml. After agitation has started, the liquid was sampled with a glass tube (5 mmϕ) at regular time intervals. Each sample was photographed with a Nikon AFM camera under a microscope. The diameters of the droplets were measured by a micrometer scale which has been photographed and enlarged under the same conditions. The number of droplets measured was one thousand[10] in all cases. The mean length diameter, the mean surface diameter, the mean volume diameter, the standard deviation, and the particle-size distribution were calculated by means of a SEIKO-301 computer.

Results and Discussion

Effect of the Viscosity Ratio, μ_d/μ_c, on the Particle-size Distribution. The particle-size distributions, calculated based on the length diameters measured at different revolution number and after 60 min of agitation, are shown in Fig. 2. In these cases, the viscosity ratio was 0.271 : 1, and the revolution rates were 330, 400, and 660 rpm. Although sufficient agitation was undertaken, the size distribution was broad and had two peaks at the revolution number of 330 and 400 rpm. The size distribution at 660 rpm, however, was normal and had only one peak.

Changes in the particle-size distribution, calculated using the length diameter measured in the course of agitation, are shown in Fig. 3. The viscosity ratio and the revolution number were 0.271 and 400 rpm respectively. The size distribution at an agitation time of 5 min spread over a wide range of particle-sizes and had three peaks. After 20 min of agitation, the size distribution had two peaks, because large particles were subdivided into small ones. The size distribution at an agitation time of 60 min was narrower than that at a shorter agitation time, but it still had two peaks.

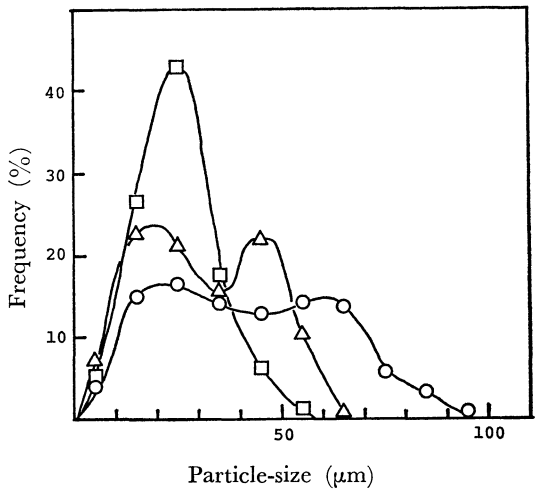

Fig. 2. Particle-size distributions at different revolution number.
D_I: 49.0 mm, D_T: 150 mm, θ: 60 min, T-20: 0.1% (w/w), μ_d/μ_c: 0.271.
○: 330 rpm, △: 400 rpm, □: 660 rpm.

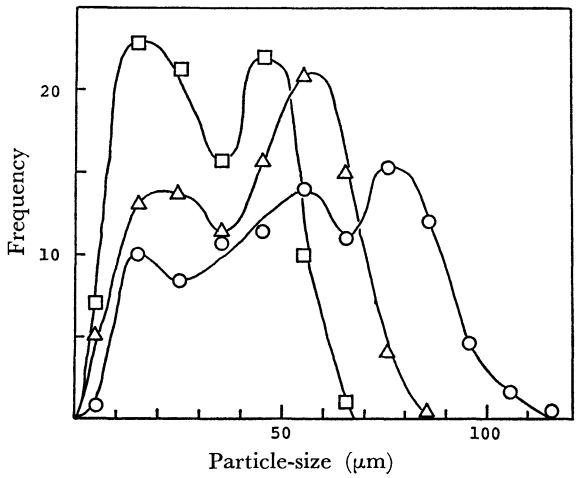

Fig. 3. Particle-size distributions at different agitation times.
D_I: 49.0 mm, D_T: 150 mm, N': 400 rpm, T-20: 0.1% (w/w), μ_d/μ_c: 0.271.
○: 5 min, △: 20 min, □: 60 min.

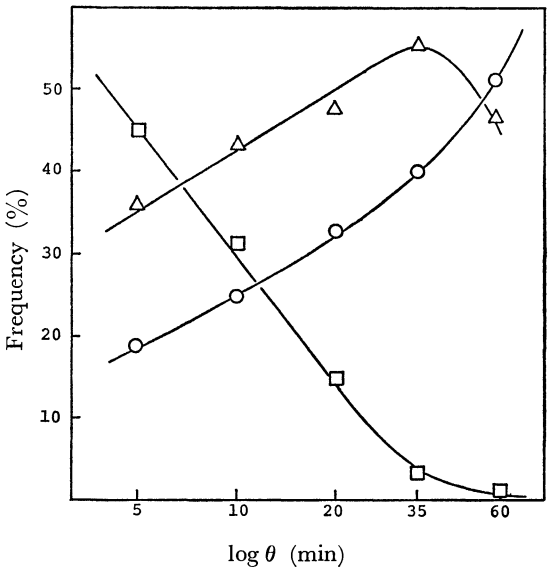

Fig. 4. Variation of frequency in the three particle-size subranges in the course of agitation.
D_I: 49.0 mm, D_T: 150 mm, N': 400 rpm, T-20: 0.1% (w/w).
○: 0—30 μm, △: 30—60 μm, □: 60 μm.

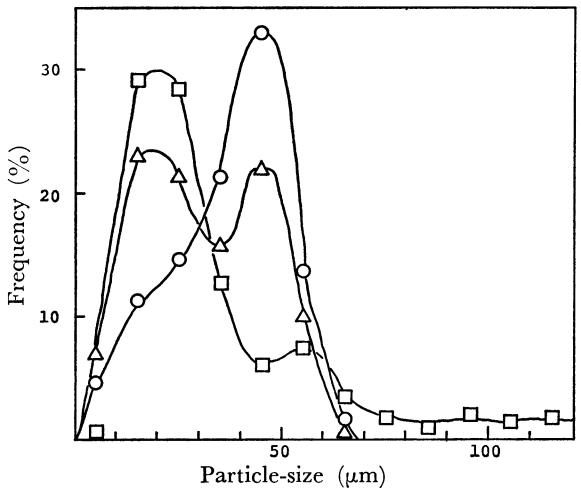

Fig. 5. Particle-size distributions at various viscosity ratios.
D_I: 49.0 mm, D_T: 150 mm, θ: 60 min, N': 400 rpm, T-20: 0.1% (w/w).
○: μ_d/μ_c=0.836, △: μ_d/μ_c=0.271, □: μ_d/μ_c= 0.00133.

In order to analyze the above results, we divided the observed particle-size range of droplets into the following three subranges: 60 μm and larger, 60 μm to 30 μm, and 30 μm and smaller. Variations in the frequency of the three subranges in the course of agitation are plotted in Fig. 4. It can clearly be observed that the frequency of droplets larger than 60 μm decreased slowly with an increase in the agitation time. On the contrary, the frequency in the middle and low subranges increased with an increase in the agitation time. However, in the middle subrange, it showed a maximum value at an agitation time of about 35 min, and then decreased.

Particle-size distributions calculated using the length diameters measured at three different viscosity ratios are shown in Fig. 5. The revolution number and the agitation time were 400 rpm and 60 μm respectively. When the continuous phase consisted of distilled water (μ_d/μ_c=0.836 : 1) alone, the size-distribution curve had only one peak. When the continuous phase consisted of a mixture of distilled water and sodium silicate (μ_d/μ_c=0.271 : 1 or 0.0133 : 1), however, the size distribution showed two peaks. On the other hand, as the viscosity ratio got smaller than unity, a broadening tendency of the size distribution was obtained. In particular, when the viscosity ratio was 0.00133 : 1, there appeared a very broad size distribution extending to the range from 70 μm to 150 μm.

Effect of the Viscosity Ratio, μ_d/μ_c, on the Mean Length Diameter. As has already been described in the section on the experimental procedure, 40 ml of an aqueous solution, a dispersed phase, was gently placed on the middle of the impeller as a globule (d_1=4.4 cm) before agitation. As soon as the agitation started, the globule was subjected to a strong shear stress in and around the impeller. Then, the globule was broken up into a number of droplets of some hundreds of microns within a few seconds. The mean length diameter of the broken-down droplets in the course of agitation at each of four different viscosity ratios was found to decrease linearly on a log-log plot, as is shown in Fig. 6. The mean length diameter was found to have the smallest value when the viscosity ratio was 0.271 : 1. In Fig. 6, the straight lines are drawn by the least-squares method. From these results, the relation between the average diameter, d_1, and the agitation time, θ, may be experimentally formulated as:

$$\log d_1 = \log \beta + \alpha \log \theta \quad (1)$$

Furthermore, the effect of the viscosity ratio on the mean length diameter at three revolution number after 60 min of agitation is given in Fig. 7. At each revolution number, the plot of the data gave a concave curve with a minimum at a viscosity ratio of 0.271 : 1. Consequently, the optimum condition for preparing an emulsion of the minimum mean length diameter would be when the viscosity of the continuous phase is slightly higher than that of water, as in Table 1. Table 3 summarizes the results of the calculations of the standard deviation, σ, of the mean length diameter and the maximum diameter of the droplets, d_m, under various conditions. As the viscosity ratio at each revolution number decreased, both σ and d_m increased. However, this trend was not observed when the continuous phase consisted of distilled water (μ_d/μ_c= 0.836 : 1) alone.

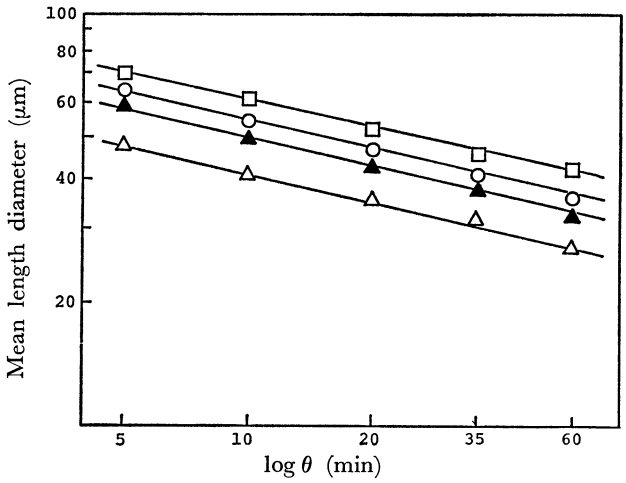

Fig. 6. Changes of the mean length diameter in the course of agitation.
D_I: 49.0 mm, D_T: 150 mm, N': 400 ppm, T-20: 0.1% (w/w).
○: μ_d/μ_c=0.836, △: μ_d/μ_c=0.271, ▲: μ_d/μ_c= 0.0280, □: μ_d/μ_c=0.00133.

Table 2. Calculated values from the plots of Fig. 6

Viscosity ratio μ_d/μ_c	Slope α	Intercept at 1 min β	Interrelation coefficient
0.836	−0.2634	2.000	0.9845
0.271	−0.1943	1.813	0.4962
0.0280	−0.2433	1.948	0.9987
0.00133	−0.2340	2.019	0.9865

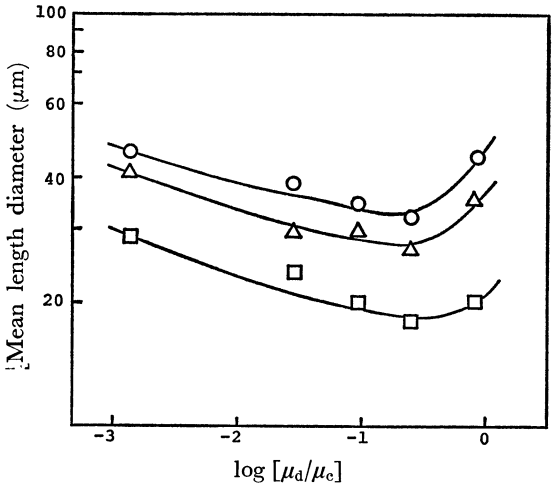

Fig. 7. Relation between the mean length diameter and the viscosity ratio.
D_I: 49.0 mm, D_T: 150 mm, θ: 60 min, T-20: 0.1% (w/w).
○: 330 rpm, △: 400 rpm, □: 660 rpm.

Table 3. Effect of experimental conditions on standard deviation and maximum diameter

Experimental conditions			Standard deviation	Maximum diameter
Viscosity ratio μ_d/μ_c	Revolution number N' (rpm)	Agitation time θ (min)	σ	d_m (μm)
0.836	330	60	13.8	200.0
0.836	400	60	10.8	100.5
0.836	600	60	5.62	53.1
0.271	330	60	20.0	84.2
0.271	400	60	12.9	59.6
0.271	660	60	6.46	32.6
0.0992	330	60	18.2	80.0
0.0992	400	60	12.7	70.2
0.0992	660	60	8.23	49.0
0.0280	330	60	20.3	93.4
0.0280	400	60	15.9	80.0
0.0280	660	60	10.0	32.4
0.00133	330	60	50.3	113.0
0.00133	400	60	41.0	195.0
0.00133	660	60	21.4	246.0

The Relation between the Specific Interfacial Energy and the Viscosity Ratio. The mean surface-volume diameter of droplets is generally represented by;

$$d_{sv} = \frac{\sum d_l^3}{\sum d_l^2} = \frac{\sum d_l^3/n}{\sum d_l^2/n} = \frac{d_v^3}{d_s^2} \quad (2)$$

where d_l is the length diameter; n, the number of droplets measured; d_s, the mean surface diameter (cm), and d_v, the mean volume diameter (cm). The specific interfacial area per 1 cm³ of the dispersed phase is given by;

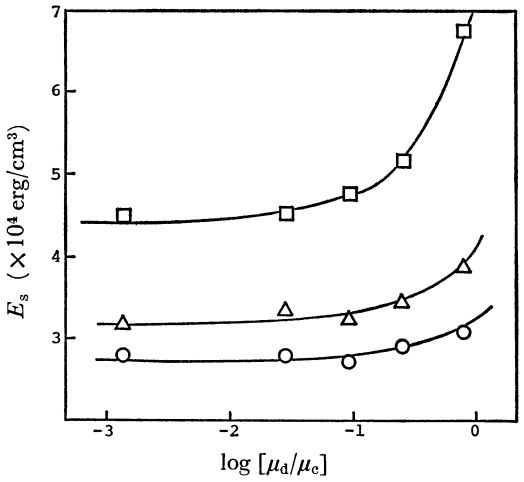

Fig. 8. Relation between the specific interfacial energy and the viscosity ratio.
D_I: 49.0 mm, D_T: 150 mm, θ: 60 min, T-20: 0.1% (w/w).
○: 330 rpm, △: 400 rpm, □: 660 rpm.

$$S = \frac{\pi \sum d_i^2}{\pi/6 \cdot \sum d_i^3} = \frac{6 d_s^2}{d_v^3} = \frac{6}{d_{sv}} \quad (3)$$

Further, the specific interfacial energy is defined as:

$$E_s = \gamma \cdot S = 6 \cdot \gamma / d_{sv} \quad (4)$$

where E_s is the specific interfacial energy (erg/cm³) and where γ is the interfacial tension (dyn/cm).

The relation between the specific interfacial energy and the viscosity ratio is shown in Fig. 8. At each revolution number, the specific interfacial energy increases remarkably as the viscosity ratio approached unity. This trend was especially notable at a high revolution number (660 rpm). Accordingly, the probability of the droplets breaking-up during agitation will increase as the viscosity ratio approaches unity.

References

1) K. J. Valentas, *I. & E. C. Fundamentals*, **5**, 271 (1966).
2) K. Shinoda and H. Arai, *J. Phys. Chem.*, **68**, 385 (1964).
3) W. A. Rodgen, V. G. Trice, and J. H. Rushton, *Chem. Eng. Progr.*, **52**, 515 (1956).
4) S. Tsukiyama and A. Takamura, *Chem. Pharm. Bull.* (Tokyo), **23**, 616 (1975).
5) S. Tsukiyama and A. Takamura, *ibid.*, **22**, 2607 (1974).
6) S. Tsukiyama, H. Takahashi, I. Takashima, and S. Hatano, *Yakugaku Zasshi*, **91**, 305 (1971).
7) S. Tsukiyama, A. Takamura, and N. Nakura, *ibid.*, **94**, 490 (1974).
8) S. Tsukiyama, A. Takamura, and M. Nakano, *ibid.*, **93**, 231 (1973).
9) S. Tsukiyama, A. Takamura, and Y. Moronuki, *ibid.*, **94**, 471 (1974).
10) H. G. Jellinek, *J. Soc. Chem. Ind.* (London), **69**, 225 225 (1950).